

Resonant electronic Raman scattering in high- T_c superconductors

E. Ya. Sherman and C. Ambrosch-Draxl

Institute for Theoretical Physics, Karl-Franzens-University of Graz, Graz A-8010, Austria

O. V. Misochko

Institute of Solid State Physics RAS, Chernogolovka, Moscow Region, 142432 Russia

(Received 19 October 2001; published 28 March 2002)

Resonant properties of Raman scattering in the superconducting state of high- T_c cuprates are considered. It is shown that the resonance between the incident light and the electronic interband transitions strongly influences the relative intensities and shapes of the Raman spectra measured in different scattering polarizations.

DOI: 10.1103/PhysRevB.65.140510

PACS number(s): 74.50.+r, 74.70.Tx, 73.40.-c, 71.28.+d

A Raman experiment measures the spectral density of the scattered light as a function of the shift between the frequencies of the incident (ω) and scattered ($\omega - \Omega$) photons, arising due to the excitation of a quasiparticle. Since the interaction between matter and light depends on ω , the probability of the excitation being ω dependent increases when the light is in resonance with electronic interband transitions. Phonon Raman scattering in high- T_c cuprates clearly demonstrates resonant behavior¹ both above and below T_c . Below T_c the Raman continuum of electronic excitations shows wide peaks, arising due to the Cooper pair-breaking Raman process.²⁻⁶ Different maxima positions in different scattering polarizations are a manifestation of the anisotropic superconducting gap. At the same time, the shape and the maximum position of these peaks in $\text{Tl}_2\text{Ba}_2\text{CuO}_{6+\delta}$,⁷ $\text{HgBa}_2\text{Ca}_2\text{Cu}_3\text{O}_{8+\delta}$,⁸ and $\text{Bi}_2\text{Sr}_2\text{CaCu}_2\text{O}_{8+\delta}$ (Ref. 9) depend on ω . The part of the spectrum at $\hbar\Omega \sim 4000 \text{ cm}^{-1}$ shows resonances too.¹⁰ The electronic structure of the high- T_c cuprates reveals a high density of bands between 2 and 3 eV below the Fermi level,¹¹ which are in resonance with the light used in Raman experiments. These theoretical and experimental observations support the importance of resonance effects. The investigation of the normal-state Raman scattering in $\text{YBa}_2\text{Cu}_3\text{O}_7$ on the basis of first-principles calculations¹² revealed an ω dependence of the continuum. Resonances in two-magnon scattering observed in $\text{YBa}_2\text{Cu}_3\text{O}_6$ ¹³ and $\text{PrBa}_2\text{Cu}_3\text{O}_7$ ¹⁴ were treated theoretically by Chubukov and Frenkel, and by Morr and Chubukov.¹⁵

The background of the current understanding of Raman scattering in BCS superconductors was established by Abrikosov and Fal'kovskii,¹⁶ Tong and Maradudin,¹⁷ Tilley,¹⁸ Cuden,¹⁹ and Klein and Dierker.²⁰ A theory of Raman scattering in d -wave-gap superconductors was proposed by Devereaux and Einzel.²¹ It was recognized that interband transitions play an important role in forming the Raman matrix element (vertex);^{19,22} however, no analysis of the resonances was given in these papers.

An unsolved problem relevant for the resonance is the intensity in the fully symmetrical A_{1g} polarization. The response to the A_{1g} perturbation is diminished by screening, while for other symmetries the effect of screening is negligibly small.^{20,22} Therefore, a relatively weak Raman intensity in the A_{1g} channel in comparison to others is expected, contrary to the experimental observations.⁶ A solution of this

controversy²³ can be attributed to the A_{1g} scattering by spin fluctuations. Since the screening is directly related to the anisotropy of the Raman process matrix element $\gamma_{\mathbf{k}}(\omega)$, the ratio of the Raman intensities in different polarizations is ω dependent if the anisotropy of $\gamma_{\mathbf{k}}(\omega)$ depends on ω .

The purpose of this paper is to consider resonance effects on the Raman peaks in a $d_{x^2-y^2}$ -gap superconductor. We will show that the experimentally observed intensity ratio in different polarizations can be explained by resonances. Below we put $\hbar \equiv 1$.

Since Raman scattering is a dissipation of the external perturbation due to the creation of excitations, the scattering efficiency is proportional to the imaginary part of the Raman susceptibility χ_R , given at temperature T in the Matsubara representation by

$$\chi_R(i\nu_n) = -T \text{tr} \sum_m \int \tilde{\gamma}_{\mathbf{k}}(\omega) \hat{G}_{\mathbf{k}}(i\omega_m) \hat{\gamma}_{\mathbf{k}}^*(\omega) \times \hat{G}_{\mathbf{k}}(i\omega_m - i\nu_n) \frac{d\xi dl_F}{(2\pi)^2}. \quad (1)$$

$\tilde{\gamma}_{\mathbf{k}}(\omega)$ is the Raman vertex "dressed" by the interactions within the system, $\omega_m = \pi T(2m+1)$ and $\nu_n = 2\pi Tn$ are the fermionic and bosonic Matsubara frequencies, respectively, and tr is the trace. $\xi = k - k_F$, k_F is the Fermi momentum, and dl_F is the Fermi-line element. The Gor'kov-Nambu Green function $\hat{G}_{\mathbf{k}}(i\omega_m)$ has the form

$$\hat{G}_{\mathbf{k}}(i\omega_m) = - \frac{i\tilde{\omega}_m \hat{\tau}_0 + v_F \xi \hat{\tau}_3 + \Delta_{\mathbf{k}} \hat{\tau}_1}{\tilde{\omega}_m^2 + v_F^2 \xi^2 + \Delta_{\mathbf{k}}^2}, \quad (2)$$

where $\hat{\tau}_i$ are the Pauli matrices, v_F is the Fermi velocity, the renormalized Matsubara frequency $\tilde{\omega}_m = \omega_m + i\Sigma(\omega_m)$, with $\Sigma(\omega_m)$ being the self-energy, and $\hat{\gamma}_{\mathbf{k}}(\omega) = \tilde{\gamma}_{\mathbf{k}}(\omega) \hat{\tau}_3$. As the source of the self-energy we consider the scattering by short-range impurities in the s channel with $\Sigma(\omega_m)$ satisfying Dyson's equation:²⁴⁻²⁶

$$\Sigma(\omega_m) = i \frac{J_m \Gamma_{\text{imp}}}{\cos^2 \delta_0 + J_m^2 \sin^2 \delta_0}, \quad J_m = \int \frac{\tilde{\omega}_m}{\sqrt{\tilde{\omega}_m^2 + \Delta_{\mathbf{k}}^2}} \frac{d\phi}{2\pi}, \quad (3)$$

where we assume $\Delta_{\mathbf{k}} = \Delta_0 \cos(2\phi)$, where Δ_0 is the gap maximum, Γ_{imp} is the relaxation rate due to impurities, δ_0 is the phase shift, and ϕ is the angle between \mathbf{k} counted from the (π, π) point and the x axis. The screening can be taken into account within the random-phase approximation:

$$\tilde{\chi}_R(i\nu_n) = \chi_{\gamma\gamma^*}(i\nu_n) - \frac{\chi_{\gamma 1}(i\nu_n)\chi_{1\gamma^*}(i\nu_n)}{\chi_{11}(i\nu_n)}, \quad (4)$$

where $\chi_{\gamma\gamma^*}(i\nu_n)$, $\chi_{\gamma 1}(i\nu_n)$, $\chi_{1\gamma^*}(i\nu_n)$, and $\chi_{11}(i\nu_n)$ are determined by the right-hand side of Eq. (1) with one or both vertices substituted by 1, and not renormalized by the Coulomb interaction. The analytical continuation $i\nu_n \rightarrow \Omega + i0$ has to be done in Eq. (1), which can be performed numerically with the Padé approximants.²⁷ At $T=0$ and $\Gamma_{\text{imp}}=0$, Eq. (1) yields the result for the polarizations B_{1g} ($\mathbf{e}_1 \parallel \hat{x} + \hat{y}$, $\mathbf{e}_S \parallel \hat{x} - \hat{y}$) and B_{2g} ($\mathbf{e}_1 \parallel \hat{x}$, $\mathbf{e}_S \parallel \hat{y}$), where \mathbf{e}_1 (\mathbf{e}_S) is the polarization of the incident (scattered) light, and \hat{x} and \hat{y} are the crystal axes,^{20,21}

$$\chi_R''(\Omega) = \frac{N_F}{\Omega} \text{Re} \left\langle \frac{|\gamma_{\mathbf{k}}(\omega)\Delta_{\mathbf{k}}|^2}{\sqrt{\Omega^2 - 4|\Delta_{\mathbf{k}}|^2}} \right\rangle. \quad (5)$$

Here N_F is the density of states at the Fermi level and $\langle \dots \rangle$ denotes averaging over the Fermi surface. In Eq. (5) the B_{1g} response diverges at $2\Delta_0$ since $\chi_R''(\Omega \rightarrow 2\Delta_0) \sim \ln|\Omega - 2\Delta_0|$.

To model the resonant Raman scattering in the CuO_2 plane we use the two-band approximation for the Raman vertex:

$$\begin{aligned} \gamma_{\mathbf{k}}^{A_{1g}}(\omega) &\propto (p_{x,\mathbf{k}}^2 + p_{y,\mathbf{k}}^2) / (\omega_{\mathbf{k}} - \omega), \\ \gamma_{\mathbf{k}}^{B_{1g}}(\omega) &\propto (p_{x,\mathbf{k}}^2 - p_{y,\mathbf{k}}^2) / (\omega_{\mathbf{k}} - \omega), \\ \gamma_{\mathbf{k}}^{B_{2g}}(\omega) &\propto 2p_{x,\mathbf{k}}p_{y,\mathbf{k}} / (\omega_{\mathbf{k}} - \omega). \end{aligned} \quad (6)$$

Here $p_{x,\mathbf{k}}$ and $p_{y,\mathbf{k}}$ are the components of the interband matrix element of momentum between the initial $E_i(\mathbf{k})$ and the final band states near the Fermi line, and $\omega_{\mathbf{k}} = E_F - E_i(\mathbf{k}) - i\Gamma_{\mathbf{k}}$ is the interband distance taken at the Fermi line including the broadening $\Gamma_{\mathbf{k}}$. Typically, the damping of the interband excitation is chosen to be \mathbf{k} independent with $\Gamma = 0.1$ eV.²⁸ The momentum dependence of $\gamma_{\mathbf{k}}(\omega)$ is due to the \mathbf{k} dependence of $p_{x,\mathbf{k}}$ and $p_{y,\mathbf{k}}$ and the interband distance $\omega_{\mathbf{k}}$. A photon probes a region where $\omega_{\mathbf{k}}$ is close to ω with an enhanced efficiency.

To obtain $\omega_{\mathbf{k}}$ and $p_{x,\mathbf{k}}, p_{y,\mathbf{k}}$ we employ the tight-binding model, which includes Cu-O2(O3) hopping $t = 1.1$ eV, O2-O3 hopping $t' = -0.40$ eV, and zero energy difference between the Cu and O orbitals. The parameters chosen allow to model simultaneously the shape of the Fermi line and the resonant properties of Raman scattering. The Fermi level intersects the upper antibonding band. The nonbonding band formed mainly by the oxygen orbitals is the initial state $E_i(\mathbf{k})$, with the interband distance $E_F - E_i(\mathbf{k})$ shown in Fig. 1. The photons with $\omega \approx 2.25$ eV are in resonance with the states near the gap maximum, while those with $\omega \approx 2.8$ eV

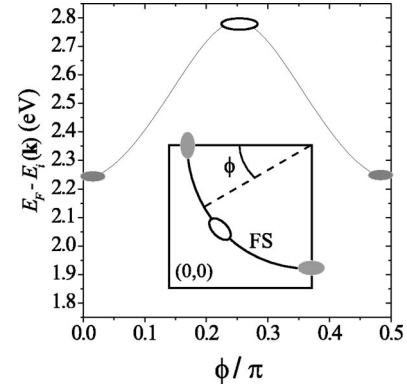


FIG. 1. The interband distance $E_F - E_i(\mathbf{k})$ and the probed regions (shown in the inset) near the Fermi line. The regions near the gap maximum (probed at $\omega = 2.25$ eV) and the gap nodes (probed at $\omega = 2.75$ eV) are marked by the gray and white ellipses, respectively.

are in resonance with the states near the gap nodes. The components of the tight-binding wave function $|\psi_{\mathbf{k}}\rangle = (\eta_{\mathbf{k}}^{[\text{Cu}]}, \eta_{\mathbf{k}}^{[\text{O2}]}, \eta_{\mathbf{k}}^{[\text{O3}]})$ correspond to atomlike orbitals. The matrix elements of $\mathbf{p}_{\mathbf{k}}$ bilinear in $\eta_{\mathbf{k}}$ were described in Ref. 29. Figure 2 shows $|\gamma_{\mathbf{k}}^2(\omega)|$ calculated for different polarizations and photon energies.

The results for $\chi_R''(\Omega)$ in the unitary limit $\delta_0 = \pi/2$ are presented in Fig. 3. The parameter Γ_{imp} was chosen to give a reliable fit to the experimental data for the B_{1g} peak, in $\text{Bi}_2\text{Sr}_2\text{CaCu}_2\text{O}_{8+x}$ ($T_c = 89$ K) obtained at $\omega = 1.95$ eV with a very low noise/signal ratio.⁹ To get the low-frequency

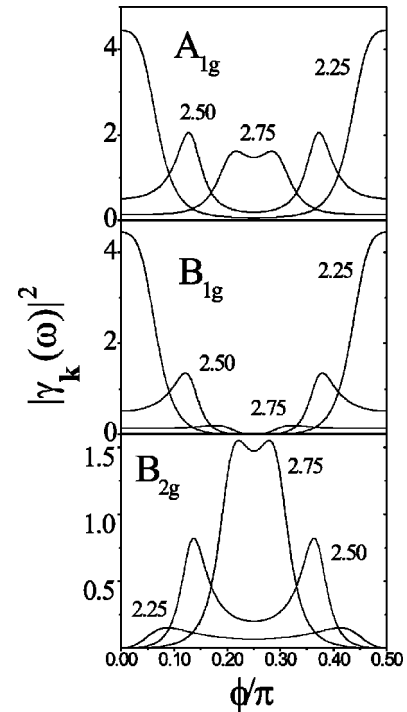


FIG. 2. $|\gamma_{\mathbf{k}}(\omega)|^2$ for different light polarizations and photon energies. Photon energies (in eV) are indicated near the lines, the lifetime is chosen to be $\Gamma = 0.1$ eV.

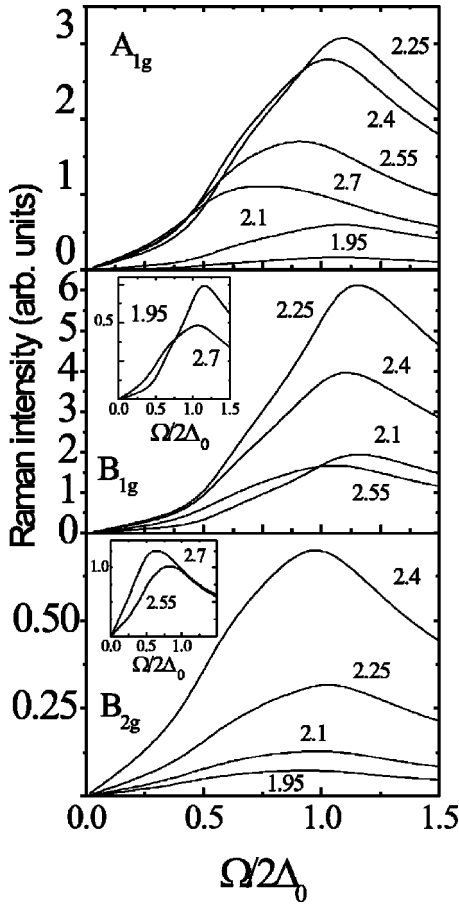


FIG. 3. Raman intensity for the A_{1g} , B_{1g} , B_{2g} polarizations in the unitary scattering limit. The photon energies (in eV) are indicated near the lines and $\Gamma = 0.1$ eV. The insets show the weakest intensities for the B_{1g} polarization and the strongest for the B_{2g} one.

slope $\chi_R''(\Omega)/\Omega$ and the width of the measured peak, one has to assume a high relaxation rate $\Gamma_{\text{imp}}/\Delta_0 = 0.35$. Figure 2 demonstrates that $\chi_R''(\Omega)$ strongly depends on ω in all polarizations. Therefore a few conclusions can be drawn.

(i) The peak positions Ω_0 for the A_{1g} ($\Omega_0^{A_{1g}}$) and B_{2g} ($\Omega_0^{B_{2g}}$) channels vary as $1.5\Delta_0 < \Omega_0^{A_{1g}} < 2\Delta_0$ and $1.3\Delta_0 < \Omega_0^{B_{2g}} < 2\Delta_0$. The B_{1g} maximum position $\Omega_0^{B_{1g}}$ is robust with respect to ω since this polarization measures effectively the density of states of the pair-breaking excitations. $\Omega_0^{B_{1g}}$ is larger than $2\Delta_0$ due to the damping of the excitations. A maximum shift of $\sim 0.1\Delta_0$ from $\omega = 2.7$ eV to $\omega = 1.95$ eV can be detected. At frequencies close to resonance with the states near the gap maximum ($\omega = 2.25$ eV), $\Omega_0^{A_{1g}}$, $\Omega_0^{B_{1g}}$, and $\Omega_0^{B_{2g}}$ become close.³⁰ The B_{1g} peak is getting sharper under this condition.

(ii) For the B_{1g} spectra the $\Omega \ll \Delta_0$ region is of special interest since it is expected to clarify the gap symmetry. Figure 2 shows that this part strongly depends on ω . In the unitary limit a crossover from $\chi_R'' \sim \Omega$ to $\chi_R'' \sim \Omega^3$ behavior is supposed to occur at $\Omega^* \sim \sqrt{\Gamma_{\text{imp}}\Delta_0}$.²⁴ The linear behavior at $\Omega \rightarrow 0$ arises due to a finite density of states $\sim N_F \sqrt{\Gamma_{\text{imp}}/\Delta_0}$ at zero excitation energy. If the states near the gap nodes are

in resonance with the interband transitions, the low-frequency behavior of $\chi_R''(\Omega)$ and the position of the crossover are determined by the \mathbf{k} dependence of both, the gap and the Raman vertex. This occurs when $\gamma_{\mathbf{k}}^{B_{1g}}(\omega)$ is strongly \mathbf{k} dependent near the nodes in the interval of angles $|\phi - \pi/4| \leq \sqrt{\Gamma_{\text{imp}}/\Delta_0}$. The angle near the Brillouin-zone (BZ) diagonals, where the dependence of the Raman vertex is weak, is of the order of $\sqrt{\Gamma/8W}$, where $W = \omega_{\mathbf{k}||(\pi,\pi)} - \omega_{\mathbf{k}||(\pi,\pi)}$. Therefore, the $\Omega \ll \Delta_0$ region becomes sensitive to the details of the Raman vertex if $\sqrt{\Gamma/W} < 2\sqrt{\Gamma_{\text{imp}}/\Delta_0}$. When the resonance is achieved near the intersection point of the BZ diagonals and the Fermi line, the linear part of $\chi_R''(\Omega)$ extends.

The evolution of the shape of the B_{1g} peak corresponds well to the experimental data on $\text{Tl}_2\text{Ba}_2\text{CuO}_{6+\delta}$ (Ref. 7) and $\text{Bi}_2\text{Sr}_2\text{CaCu}_2\text{O}_{8+\delta}$.⁹ In these studies the region of $\chi_R''(\Omega)$ linear in Ω increased, the peak became broader, and the maximum position was shifted by about $0.1\Delta_0$ with increasing ω . However, in Ref. 9, where the maximum position was quantitatively investigated, the maximum was shifted to lower frequencies, in contrast to our results. The reason for this discrepancy will be discussed later. At the same time, the results on $\text{HgBa}_2\text{Ca}_2\text{Cu}_3\text{O}_{8+\delta}$ (Ref. 8) show a behavior corresponding to our approach: with the extension of the linear region and broadening, the maximum shifts to lower frequencies. However, this occurs when $\omega_{\mathbf{k}||(\pi,\pi)} > \omega_{\mathbf{k}||(\pi,\pi)}$ corresponding to $t'/t > 0$ in the tight-binding model. One may conclude that in this compound, the states that have large $|\mathbf{p}_{\mathbf{k}}|$ for the transitions to the Fermi line have a different dispersion than those in the Bi- and the Tl-based materials.

(iii) Close intensities in the B_{1g} , B_{2g} , and A_{1g} polarizations observed experimentally can be achieved at the resonance near the BZ diagonals. The A_{1g} intensity is expected to be smaller than the B_{1g} one due to the screening, which suppresses the A_{1g} response up to an order of magnitude. The B_{2g} scattering is diminished since $\gamma_{\mathbf{k}}^{B_{2g}}(\omega) = 0$ at the BZ boundaries, where the density of states for the pair-breaking excitations is maximal. Due to the resonance, the peak intensities can get closer. For the A_{1g} polarization the intensity is enhanced by the anisotropy of the Raman vertex. For the B_{2g} polarization a large contribution of the states near the gap nodes enhances $\chi_R''(\Omega)$. The Raman vertex can be expanded as the sum of the Fourier harmonics as $\gamma_{\mathbf{k}}(\omega) = \sum_l \gamma_l(\omega) \cos l\phi$ or $\gamma_{\mathbf{k}}(\omega) = \sum_l \gamma_l(\omega) \sin l\phi$. If the resonance is achieved near the high-symmetry directions (k, k) or $(k, 0)$, the sum contains components up to $l_{\text{max}} \sim \sqrt{W/\Gamma}$, while for the resonance far from the high-symmetry lines $l_{\text{max}} \sim W/\Gamma$.

Now we can address the role of the lifetime Γ . Analysis of the Raman process shows that the dependence of $\chi_R''(\Omega)$ on Γ becomes considerable if the resonance is achieved near the BZ diagonals, and the maximum position can be shifted due to the \mathbf{k} dependence of Γ . Therefore, the experimentally observed shift in the peak position to higher frequencies with the increase in ω can be due to the \mathbf{k} dependence of the lifetime, which was not taken into account here. Another reason can be more fundamental and related to the gap maxi-

mum achieved not at the BZ axes but at other \mathbf{k} directions, which does not contradict the $d_{x^2-y^2}$ -gap symmetry. In this case $|\Delta_{\mathbf{k}}|$ should have eight equivalent maxima.

We assumed above that the pair-breaking process is a major contribution to the A_{1g} scattering, which under resonant conditions has an intensity close to that of the B_{1g} channel. However, this contribution might be not unique. For example, the nonscreened spin fluctuations can contribute to the A_{1g} response, shifting the observed peak position to a frequency close to that observed in the inelastic neutron-scattering experiments.³¹

To conclude, we calculated the dependence of the shape and the intensity of the pair-breaking peaks in the electronic

Raman scattering in a $d_{x^2-y^2}$ -gap superconductor on the exciting light frequency. The position of the B_{1g} peak is robust with respect to the photon frequency with a possible shift of the order of $0.1\Delta_0$. The experimentally observed close intensities in the A_{1g} , B_{1g} , and B_{2g} channels hint on the interband resonance achieved near the gap nodes. The systematic studies of the resonant dependences in the absolute values of the intensities are crucially desired in this field.

The authors acknowledge support from the Austrian Science Fund via Project No. M591-TPH (E.Y.S.) and from the Russian Foundation for Basic Research (Grant No. 01-02-16480 for O.V.M). E.Y.S. is grateful to A. Sacuto and Y. Gallais for very interesting discussions.

-
- ¹O.V. Misochko *et al.*, Phys. Rev. B **59**, 11 495 (1999).
²T.P. Devereaux *et al.*, Phys. Rev. Lett. **72**, 396 (1994).
³X.K. Chen *et al.*, Phys. Rev. Lett. **73**, 3290 (1994).
⁴T. Strohm and M. Cardona, Phys. Rev. B **55**, 12 725 (1997).
⁵L.V. Gasparov *et al.*, Phys. Rev. B **55**, 1223 (1997).
⁶Electronic Raman results on high- T_c cuprates have been reviewed by R. Hackl, in *The Gap Symmetry and Fluctuations in High- T_c Superconductors*, edited by J. Bok *et al.* (Plenum Press, New York, 1998), Vol. 249; A. Bock, Ann. Phys. (Leipzig) **8**, 441 (1999); M. Cardona, Physica C **317-318**, 30 (1999).
⁷M. Kang *et al.*, Phys. Rev. Lett. **77**, 4434 (1996).
⁸A. Sacuto, *et al.*, Phys. Rev. B **58**, 11 721 (1998).
⁹O.V. Misochko and E.Ya. Sherman, J. Phys.: Condens. Matter **12**, 9095 (2000).
¹⁰M. Rübhausen, *et al.*, Phys. Rev. B **56**, 14 797 (1997).
¹¹O.K. Andersen *et al.*, J. Phys. Chem. Solids **56**, 1573 (1995).
¹²S.N. Rashkeev and G. Wendin, Phys. Rev. B **47**, R11 603 (1993).
¹³G. Blumberg *et al.*, Phys. Rev. B **53**, R11 930 (1996).
¹⁴M. Rübhausen *et al.*, Phys. Rev. B **53**, 8619 (1996).
¹⁵A.V. Chubukov and D.M. Frenkel, Phys. Rev. Lett. **74**, 3057 (1995); D.K. Morr and A.V. Chubukov, Phys. Rev. B **56**, 9134 (1997).
¹⁶A.A. Abrikosov and L.A. Fal'kovskii, Zh. Éksp. Teor. Fiz. **40**, 262 (1961) [Sov. Phys. JETP **13**, 179 (1961)].
¹⁷S.Y. Tong and A.A. Maradudin, Mater. Res. Bull. **4**, 563 (1969).
¹⁸D.R. Tilley, Z. Phys. **254**, 71 (1972); D.R. Tilley, J. Phys. F: Met. Phys. **3**, 1417 (1973).
¹⁹C.B. Cuden, Phys. Rev. B **13**, 1993 (1976); **18**, 3156 (1978).
²⁰M.V. Klein and S.B. Dierker, Phys. Rev. B **29**, 4976 (1984).
²¹T.P. Devereaux and D. Einzel, Phys. Rev. B **51**, 16 336 (1995).
²²A.A. Abrikosov and V.M. Genkin, Zh. Exp. Theor. Fiz. **65**, 842 (1973) [Sov. Phys. JETP **38**, 417 (1974)].
²³F. Venturini *et al.*, Phys. Rev. B **62**, 15 204 (2000).
²⁴T.P. Devereaux, Phys. Rev. Lett. **74**, 4313 (1995).
²⁵C. Jiang and J.P. Carbotte, Phys. Rev. B **53**, 11 868 (1996).
²⁶V. P. Mineev and K. Samokhin, *Introduction to Unconventional Superconductivity* (Gordon and Breach, New York, 1999).
²⁷H.J. Vidberg and J.W. Serene, J. Low Temp. Phys. **29**, 179 (1977).
²⁸E.T. Heyen *et al.*, Phys. Rev. Lett. **65**, 3048 (1990).
²⁹E.Ya. Sherman and C. Ambrosch-Draxl, Solid State Commun. **115**, 669 (2000); Phys. Rev. B **62**, 9713 (2000).
³⁰Since the band structure depends on the doping, the resonant properties of the Raman spectra depend on the doping as well. For this reason, the coalescence of the peaks in different polarizations with the change of the doping [C. Kendziora, R.J. Kelley, M. Onellion, Phys. Rev. Lett. **77**, 727 (1996)] might be attributed to the change of the resonant conditions.
³¹Y. Gallais *et al.*, cond-mat/0108015, Phys. Rev. Lett. (to be published 2002).